Geochimica et Cosmochimica Acta 403 (2025) 240–251

Contents lists available at ScienceDirect

Geochimica et Cosmochimica Acta

journal homepage: www.elsevier.com/locate/gca

Limited mercury (Hg) partitioning into bitumen and efficient gaseous Hg reabsorption during early thermal maturation of organic-rich mudrocks

Asri O. Indraswari [a,b,*], Joost Frieling [a], Erdem Idiz [a], Tamsin A. Mather [a], Hugh C. Jenkyns [a], Stuart A. Robinson [a], Alexander J. Dickson [c]

[a] Department of Earth Sciences, University of Oxford, South Parks Road, Oxford OX1 3AN, UK
[b] Department of Geosciences, Faculty of Mathematics and Natural Sciences (FMIPA), Universitas Indonesia, Depok 16424, Indonesia
[c] Centre of Climate, Ocean and Atmosphere, Department of Earth Sciences, Royal Holloway University of London, Egham, Surrey TW20 0EX, UK

ARTICLE INFO

Associate editor: Jiu bin Chen

ABSTRACT

Recent studies have looked into the impact of exposure to extremely high temperature, such as typifies contact metamorphism, on mercury (Hg) distributions in sediments, and observed significant Hg loss with increasing temperature. By contrast, sediment cores of Lower Jurassic organic-rich Posidonienschiefer (also known as Posidonia Shale) from the Lower Saxony Basin, Germany seemingly showed Hg enrichment after maturation related to basin subsidence and burial under more typical geothermal gradients. To investigate the apparent differences in Hg behaviour, we conducted a series of artificial maturation experiments on immature Posidonienschiefer samples, analysing Hg concentrations within rock residues and bitumen generated during early maturation stages. Thermal desorption profiles were used to track Hg speciation changes in the matured sediment. Our results show a progressive decrease in Hg concentrations in sediments with increasing thermal maturity throughout the experiments, which dominantly relates to released gaseous Hg with only a fraction of the Hg being partitioned into the bitumen (≤1% of the total initial Hg). Further experiments showed that gaseous Hg in closed vessels was rapidly (≤1 h) and efficiently (≥95 %) reabsorbed into the sediment during cooling. We speculate that our experiments may simulate some of the processes that drive Hg mobilisation and recapture occurring in contact aureoles, such as the rapid release and recapture of gaseous Hg. However, the Hg speciation changes that occur in our experiments and during natural burial maturation clearly differ. Specifically, the changes in Hg speciation in the natural system with burial-related maturation suggest that under those conditions organic matter associated Hg may instead transition into more thermally stable phases.

1. Introduction

Understanding the processes associated with Hg behaviour during thermal evolution of sediments is key to understanding Hg more broadly in the subsurface and in mobile fluids, (e.g., in hydrocarbon reserves, Bryndzia et al. (2022)). It also pertains to the use of Hg concentrations in the sedimentary record as a proxy for large igneous province (LIP) volcanism (e.g., Sanei et al., 2012; Percival et al., 2015, 2021; Grasby et al., 2019; Indraswari et al., 2024) and aids in reconstructing Hg emissions from volcanic activity, especially those resulting from contact metamorphism of intruded sediments (Svensen et al., 2023a; Fendley et al., 2024; Frieling et al., 2025).

Sediments rich in labile organic matter undergo chemical changes in response to burial-related heating in basins, often resulting in the production of hydrocarbons, through the process of thermal maturation (Tissot & Welte, 1984; Peters et al., 2004; Dembicki, 2022). Organic matter (OM) has been widely recognised as the dominant carrier of Hg in the water column and sediments (Wallace, 1982; Benoit et al., 2001; Outridge et al., 2007), although other phases, such as metal sulfides (e.g., pyrite, (meta-)cinnabar HgS) and clay associations, may be important in the rock record (Percival et al., 2018; Shen et al., 2019, 2020; Frieling et al., 2024). Because of its high affinity with OM, Hg concentrations are typically normalised to total organic carbon (TOC) to account for increases linked to higher OM content when identifying anomalous Hg loading in sedimentary deposits (e.g., Grasby et al., 2019; Sanei et al., 2012). As Hg is commonly associated with organic matter upon deposition, which is transformed during thermal maturation, this process may result in re-distribution of Hg between solid and fluid phases, and

* Corresponding author at: Department of Geosciences, Faculty of Mathematics and Natural Sciences (FMIPA), Universitas Indonesia, Depok 16424, Indonesia.
E-mail address: asrioktavioni@ui.ac.id (A.O. Indraswari).

https://doi.org/10.1016/j.gca.2025.07.001
Received 22 October 2024; Accepted 2 July 2025
Available online 5 July 2025

potentially mobilises Hg that may facilitate transport out of the host rock. Previous studies have shown that thermal maturation of sediments with labile organic matter produces fluids, both hydrocarbon and non-hydrocarbon, into which metals such as Mo, Zn, U, and Cd have minor partitioning (Dickson et al., 2020, 2022). Similarly, only limited concentrations of Hg have been found in crude oils and hydrocarbon gases with most values falling between 1 and 20 ppb (Wilhelm et al., 2007; Wilhelm and Bloom, 2000), with some exceptions (e.g., 593 ppb in condensate liquids in Thailand; Wilhelm et al. 2007). These Hg concentrations are below those typically found in bulk average shale (~62 ppb, Grasby et al. 2019). As a result, the Hg/TOC ratio of hydrocarbons (≤0.24 ppb/%, given that hydrocarbons contain 82–87 % carbon by weight, Berkowitz, 1997) is significantly lower than that of average shales (72 ppb/% Hg/TOC; Grasby et al., 2019). However, we note that the shale average is partly derived from datasets representing periods of large igneous province (LIP) volcanism, during which Hg concentrations may be elevated (e.g. Grasby et al., 2019). Although metallic Hg has been encountered during the production of gases from well-established hydrocarbon fields (e.g., the Rotliegend reservoirs from the Netherlands and Northern Germany), the association of Hg in hydrocarbon fluids that are generated and expelled from organic-rich sediments is still not well understood (see e.g., Grotewold et al., 1979; Zettlitzer et al., 1997).

Thermal maturation of labile sedimentary OM can occur due to increasing temperature with increasing burial depth, with average temperature gradients for sedimentary basins typically ranging between 20 °C km^{-1} and 40 °C km^{-1} (Gluyas & Swarbrick, 2021). Through the process of thermal cracking, sedimentary OM (kerogen) is broken down into lower molecular weight hydrocarbon phases, such as oil and gas, often beginning at around 100–120 °C at geological heating rates (Tissot & Welte, 1984; Peters et al., 2004; Dembicki, 2022). The kerogen becomes more thermally mature as it experiences continued burial and exposure to higher temperatures within the basin and can eventually end up as a carbon-rich graphitic residue, having lost most of its labile OM as separate hydrocarbon phases. This transformation of OM during maturation raises intriguing questions regarding the fate of Hg, which has a high affinity with OM, particularly whether Hg remains associated with the original phase in which it was deposited.

There are several previous studies investigating how thermal maturation has influenced sedimentary Hg concentrations (Table 1) (Li et al., 2016; Liu et al., 2022; Chen et al., 2022; Svensen et al., 2023a; Indraswari et al., 2024). The various studies yielded insights for Hg and hydrocarbon systematics but particularly for Hg release associated with LIP volcanism. LIP-associated Hg release has been proposed to result from a combination of emissions from the magma itself and, in some cases, crustal rocks such as coals and shales that were heated directly by the LIP intrusions or by associated thermal anomalies affecting whole basins as a result of crustal thinning (Jones et al., 2019; Svensen et al., 2023a, 2023b). The observations from artificial maturation (pyrolysis) experiments at various temperatures, as well as from field studies of contact aureoles, show that rapid heating linked to igneous intrusion in general can cause significant, and potentially complete, Hg loss from sediments (Liu et al., 2022; Svensen et al., 2023a). Quantifying these processes is important in terms of the use of the Hg proxy and what it tells us about LIP-driven perturbations of the global carbon cycle (Svensen et al., 2023a; Fendley et al., 2024; Frieling et al., 2025). As a consequence, most previous studies have focused on replicating thermal conditions relevant to contact metamorphism and thermal anomalies from igneous intrusions, involving steep heating rates to a very high final temperatures (up to a maximum temperature of 750 °C) (Table 1).

In contrast to igneous intrusions, thermal maturation related to basin subsidence generally occurs in a lower (maximum) temperature regime (70–260 °C) and over much longer periods of time (commonly millions of years), resulting in the conversion of whole stratigraphic sequences of organic-rich sediments (Tissot & Welte, 1984; Gluyas & Swarbrick, 2021). The associated conversion of the organic matter (kerogen) into large volumes of hydrocarbon (oil and gas) and non-hydrocarbon (CO_2, H_2S, N_2) fluids may have a significant role in the release, mobilisation and further sequestration of Hg: processes that are not well understood to date. The contrast between apparent increases in Hg with maturation during burial (Indraswari et al., 2024) and Hg loss in most pyrolysis experiments and field observations from contact aureoles may be attributed to the different experimental conditions (open *vs* closed, isothermal *vs* non-isothermal) and the high temperatures (up to 700 °C) the samples were subjected to in the laboratory or in contact metamorphic aureoles (Fig. 1).

To improve understanding of the impact of maturation and redistribution of Hg between solid and fluid phases, we performed isothermal artificial maturation experiments to more closely simulate the process of organic-matter transformation and hydrocarbon generation (Lewan et al., 1979), especially in the initial-to-peak generation stages where significant liquid hydrocarbons are mobilised. These experiments were designed to investigate the effects of kerogen conversion and the specific physicochemical conditions that influence sedimentary Hg behaviour (Fig. 1). In natural settings, kerogen cracking and conversion to hydrocarbons is a function of heating time and temperature (Burnham, 2017), occurring over millions of years at slow heating rates. However, such timescales are impractical for laboratory studies. Therefore, elevated temperatures are widely employed in artificial maturation experiments to accelerate reaction kinetics while preserving the fundamental pathways of organic matter transformation (e.g., Lewan, 1979). In our study, the applied time–temperature conditions follow established protocols shown to reproduce the chemical evolution of kerogen and hydrocarbon formation observed in natural systems (e.g., Dickson et al., 2020). The maturation experiments in this study aimed at producing hydrocarbons generally require a compromise between practical (fast) heating times (weeks) combined with the lowest temperatures that still result in appreciable OM conversion (≥300 °C).

We performed isothermal pyrolysis experiments at 325 °C, using established protocols (see Dickson et al. 2020) for periods of up to 5 weeks, using sediment samples rich in immature labile organic matter, reaching conditions that simulate levels of early thermal maturation stages in sedimentary basins. Mercury concentrations and Hg/TOC

Table 1
Summary of temperature conditions of previous studies of the relationship between thermal maturation and sedimentary Hg concentrations.

Author(s)	Method	Temperature	Maturation Time	Final maturity reached (max %Ro)	Hg concentration final condition (maximum change %)
Liu et al., 2022	Experimental	240–610 °C	10–28.5 h	up to 3.27 %	−99
Chen et al., 2022	Experimental, high pressure (0.3 GPa)	50–700 °C	18 h	Unknown	−76
Svensen et al., 2023a	Observations from contact aureoles	215–750 °C (modelled temperature)	up to millennia for thick sills	up to 5 %	−100 (dyke) −90 (sill)
Indraswari et al., 2024	Observations from burial natural cores	70–260 °C (modelled temperature)	90 Ma	3.5 %	+302
This study	Experimental	325 °C	24–840 h	~0.88 %	−62

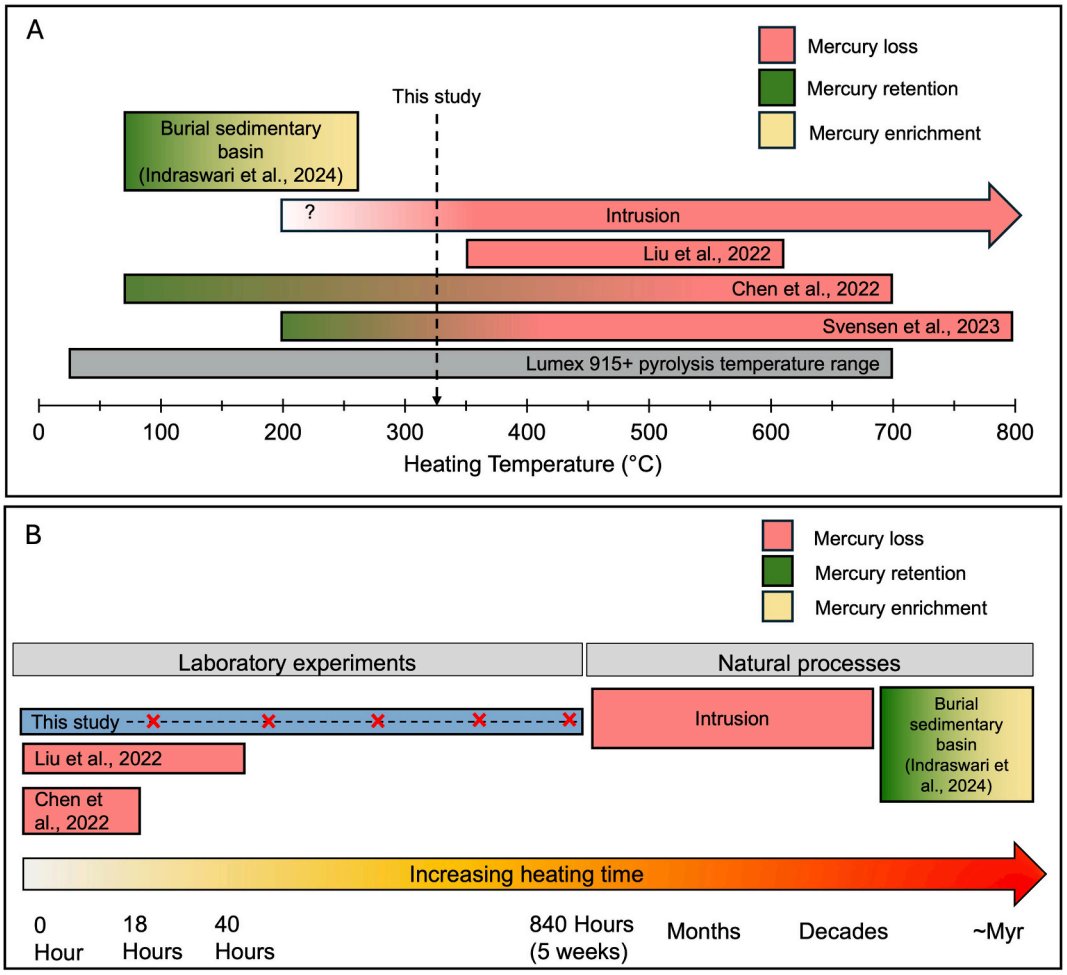

Fig. 1. (A) The context of this study compared to other previous studies looking at the effect of thermal maturation on sedimentary Hg, focusing on the influence of experimental temperature. (B) As panel A, for heating time. Mercury loss, retention, and enrichment represent the observed effects on sedimentary mercury (Hg) after experiments or geological processes, relative to its initial concentration in the sediment.

values from bulk immature samples were measured before the pyrolysis experiments. We then measured both these parameters in bulk and solvent-extracted residues as well as Hg thermal desorption profiles (Frieling et al., 2024) to track changes in Hg speciation. The differences between the parameters measured in the original immature samples and the matured pyrolysis samples were examined to determine the change in the bulk Hg concentrations and Hg/TOC values. Finally, Hg has been hypothesised to be recaptured into secondary host phases or reprecipitate with sulfides at lower temperature after mobilisation (Bryndzia et al., 2022; Frieling et al., 2025; Indraswari et al., 2024). We therefore also performed a small number of experiments whereby closed pyrolysed samples were left to cool for a short while (1–60 min) before opening to test whether Hg recapture had occurred.

2. Materials & Methods

2.1. Sample material

This study used one sample (ca. 25 g) from immature, organic matter-rich Lower Jurassic Posidonienschiefer from the Lower Saxony Basin (drill Core A in Indraswari et al., 2024). The immature sample material was taken at a relative depth of 34.65 m in core A, homogenised, and divided into ~ 1 g sub-samples for the experiments. The Posidonienschiefer, a well-known hydrocarbon source rock, is thought to have been deposited in an anoxic marine environment, locally euxinic in nature (Röhl et al., 2001; Schmid-Röhl et al., 2002; Frimmel et al., 2004; Schwark & Frimmel, 2004; Gorbanenko & Ligouis, 2014, 2015; Song et al., 2017; Celestino, 2019). The selected sample has a total organic carbon (TOC) value of 8.85 wt% and a hydrogen index (HI) of 701 mgHC/g TOC. Rock-Eval derived T_{max} values of 437 °C (vitrinite reflectance equivalent of 0.5 % Ro), puts them in the immature to earliest stage of hydrocarbon generation.

2.2. Solvent extraction

To obtain an accurate estimate for the amount of generated hydrocarbons during artificial maturation, all sediment aliquots were solvent-extracted prior to pyrolysis to remove any pre-existing bitumen fraction that might complicate quantification of the newly generated bitumen. The newly generated hydrocarbon fraction was isolated by a second solvent extraction using the same procedure after pyrolysis. The solvent-extractable organic-matter fraction from the sediments was obtained via microwave-sonication using an Analytix Advanced Microwave Digestion System at the University of Oxford following methods described in O'Connor et al. (2019). Sediment powders (~1 g dry mass) from both the original bulk samples and the post-pyrolysis residues were extracted using 20 mL of 9:1 (volume/volume) dichloromethane (CH_2Cl_2, hereafter DCM): methanol (hereafter MeOH). The microwave temperature settings were configured to gradually rise from room temperature to 70 °C in 10 min, isotherm at 70 °C for 10 min, and then decrease to 25 °C over 20 min. After centrifugation, the extracted rock residues were separated from the extracts and dried under a gentle N_2 stream. The total

lipid extracts (TLE, will hereafter be referred to as 'bitumen' throughout this paper) were then set aside and dried under N_2 and weighed. The bitumen was re-dissolved and homogenised in DCM:MeOH (9:1) prior to Hg analyses. The extraction typically yielded between 8 and 10 mg of bitumen per gram of sediment. After two microwave extraction cycles, no significant additional yield ($\leq$ 1 mg) was observed, indicating that the extraction process had reached its optimal efficiency.

2.3. Pyrolysis experiments

The pyrolysis experiments were performed in glass Carius tubes using established procedures (Tannenbaum & Kaplan, 1985; Lu & Kaplan, 1989; Dickson et al., 2020). Carius tubes were initially sterilized at 500 °C in a furnace overnight before soaking in hot 10 % HNO_3 and rinsed with hot ultra-pure 18.2 MΩ cm water. The dry extracted rock residues (~1 g) were loaded into clean Carius tubes. Each Carius tube was connected to a vacuum extraction line and flame-sealed after the internal pressure was reduced to 10^{-2} atm. While the pressure used in these experiments is not representative of the conditions that these rocks would experience in a real geological setting, a low pressure was selected specifically to minimize oxidation and combustion, and also because pyrolysis reactions produce gases, which could lead to tube rupture if high pressure were allowed to build up. The tubes were then loaded into stainless steel containment vessels for heating.

The experiments were carried out under isothermal conditions, with each sub-sample subjected to heating at 325 °C for either 24 h (1 day), 168 h (7 days), 336 h (2 weeks), 500 h (3 weeks) or 840 h (5 weeks) (Fig. 2). We selected an isothermal temperature of 325 °C based on established artificial maturation protocols, which aim to replicate the thermal breakdown of labile organic matter (kerogen) into bitumen and gas within feasible laboratory timescales. This temperature and approach are consistent with previous work (e.g., Dickson et al., 2020), where isothermal heating enables better control of reaction kinetics and product characterization. Each experiment was performed in triplicate to assess reproducibility. The experimental conditions are shown in Table 1. Upon removal from the furnace, Carius tubes were taken from their stainless-steel jackets and broken open immediately to allow the gaseous component to escape. Microwave-sonication extraction was then carried out (described in §2.2) to remove any solvent-extractable organic matter (bitumen) evolved during pyrolysis. The extracted rock residues were dried under a stream of N_2 to remove any remaining solvents and re-homogenised before Hg and Rock-Eval measurements were made (for details see §2.5 and 2.6).

2.4. Cooling and reabsorption experiments

To assess the reabsorption or uptake of generated volatile Hg compounds as a result of cooling to ambient temperature, four sample aliquots were heated in the furnace for 24 h and then left to cool in a fume hood for variable amounts of time (1, 4, 16, and 60 min) before being opened (Fig. 2). For each sub-sample, the temperature of the tube at the time of opening was measured using an infrared thermometer. The specific conditions for cooling time and opening temperature are detailed in Table 3. After opening, microwave-sonication extraction, Hg measurements, and Rock-Eval analysis were performed as described above.

2.5. Total organic carbon and Rock-Eval analysis

The amount, composition and thermal maturity of the organic matter in bulk rocks and solvent-extracted bulk rocks was characterised prior to pyrolysis using a Rock-Eval 6 at the University of Oxford (cf., Behar et al., 2001) (Fig. 2). After pyrolysis and subsequent solvent-extraction, sub-samples of residues were measured in Rock-Eval in duplicate, and the precision of the measurements was monitored using in-house standard SAB134 (Lower Jurassic organic-rich marl from St. Audries Bay, Somerset, UK, 2.7 wt% TOC) for every 8 to 10 samples. The standard deviation of the in-house standard over the period of analysis (SAB134)

Table 2
Sub-sample information and specific experimental conditions during pyrolysis experiments.

Sub-sample ID	Rock type	Temperature (°C)	Pressure (atm)	Heating time (hours)
PS-0 (Bulk rock)	Black shale	20	1	0
PS-1	Black shale	325	0.01	24
PS-2	Black shale	325	0.01	24
PS-3	Black shale	325	0.01	168
PS-4	Black shale	325	0.01	336
PS-5	Black shale	325	0.01	500
PS-6	Black shale	325	0.01	840

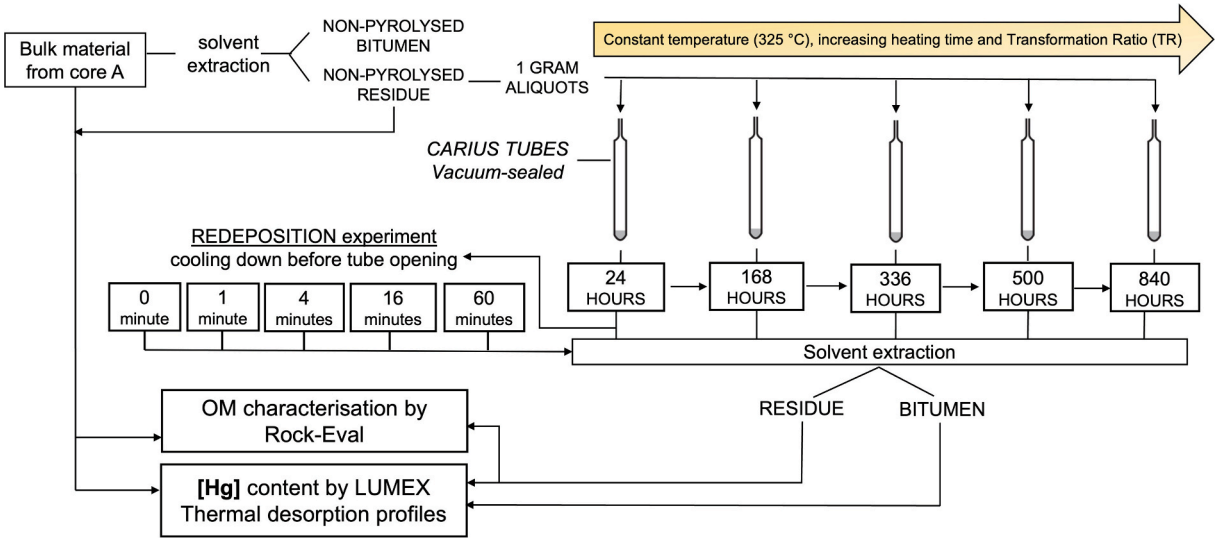

Fig. 2. Overview of the experimental procedures and analytical approaches in this study modified from Dickson et al. (2020).

Table 3
Sub-sample information and specific experimental conditions during cooling and reabsorption experiments.

Sub-sample ID	Heating time (hours)	Cooling time (minutes)	Opening temperature (°C)
R-0	24	0	280
R-1	24	1	211
R-4	24	4	63
R-16	24	16	16
R-60	24	60	16

was ± 0.03 wt% TOC.

2.6. Mercury analyses for sediments and bitumen

Mercury (Hg) analyses were conducted with a Lumex RA 915 M device, attached to a pyrolysis unit (PYRO-915+) at the University of Oxford (Bin et al., 2001). Powdered solvent-extracted and unextracted sediments of ~ 50 ± 5 mg were introduced into sample boats, heated from room temperature (~20 °C) to ~ 700 °C and left for up to 120 s to fully volatilise the Hg present. The instrument was calibrated before each run using NIST-SRM2587 (National Institute of Standards and Technology – Standard Reference Material: Trace Elements in Soil Containing Lead from Paint) with a Hg concentration of 290 ± 9 ppb. The long-term accuracy of the Hg concentration measurements, based on the SRM2587 standard, was ± 5 % of the measured value. The manufacturer-specified detection limit for the Lumex RA 915 M is ~ 0.1 ng Hg.

Mercury concentrations of Lower Saxony Basin oils sourced from the Posidonienschiefer were previously measured by Indraswari et al. (2024) on samples obtained from the Lower Saxony Oil Museum (Stock & Littke, 2016). Mercury concentrations in the bitumen were analysed using a Lumex RA-915 M instrument using similar methods as those used to analyse the oils, as described in Indraswari et al. (2024). Following pyrolysis, the solvent-extractable fractions (bitumen) were isolated (§2.2), dried under a N_2 stream and the solvent-free weight of the bitumen from each sub-sample was measured. Prior to Hg analyses, the bitumen was redissolved and homogenised in a mixture of DCM:MeOH (9:1). An aliquot of 250 μL of the diluted bitumen was pipetted into a quartz boat, dried with nitrogen (N_2), and subsequently weighed before adding a food-grade activated charcoal bed to prevent generated smoke affecting the Hg analyses. Mercury concentrations in the activated charcoal were analysed to correct for trace amounts of Hg present in the bitumen. Repeat measurements of the charcoal (n = 15) showed an average concentration of 0.4 ± 0.07 ppb (standard error of the mean), or 0.04 ± 0.007 ng Hg for a 100 mg charcoal bed. Finally, we analysed Hg concentrations in the bitumen for each sub-sample in duplicate and subtracted the trace amounts of Hg added by the charcoal bed to obtain an accurate estimate of Hg in the bitumen fraction.

2.7. Thermal desorption

Mercury thermal desorption profiles (TDPs) were generated for all sub-samples (n = 7) with duplicates and compared with TDPs from a selection of naturally matured samples in the Posidonienschiefer from Core B (n = 5) and C (n = 5) (Indraswari et al., 2024). The samples taken from Cores B and C are close stratigraphic equivalents to the bulk rock sample (PS-0) from Core A used in the pyrolysis experiments (all within ± 1 m from a relative depth of 34.65 m). The TDPs were obtained using a Lumex RA-915 M set up with a PYRO-915+ at the University of Oxford, following methods described in Frieling et al. (2024). The desorption profiles were obtained concurrently with the total mercury concentration measurements within the pyrolysis chamber in Mode 1 (rapid heating from ~ 20 to ~ 700 °C). Compared to traditional temperature ramp measurements this more rapid approach limits the influence of analytical noise, which allows us to assess and quantify Hg speciation changes for sediment samples with very low Hg concentrations (<5 ppb). Results are directly comparable to previous studies that have applied the same approach (Frieling et al., 2024, 2025). The weight of each sample was held constant at 50 ± 5 mg to avoid the effects of variable sample mass.

3. Results

3.1. Organic-matter maturation

The results of the bulk organic geochemical measurements are shown in Fig. 3. The decrease in hydrogen index (HI) from 701 to 317 mgHC/gTOC in the extracted residues (a 55 % loss) (Fig. 3A, B) highlights the increasing conversion of the kerogen as a result of maturation. The highest T_{max} of 443 °C, and the HI of 323 mgHC/g TOC in sub-sample PS-6 (840 h heating time) makes it equivalent to the naturally matured Posidonienschiefer in the Harderode Well in the Hils Syncline, Northern Germany with a measured vitrinite reflectance of ~ 0.88 % Ro (Poetz et al., 2014). The maturity levels of the pyrolysis samples range from immature to the early/peak-oil window stages of kerogen conversion. A simplified transformation ratio (TR), defined as $[(HI_{original}–HI_{measured})/HI_{original}]$, was used to calculate the proportion of HI change from the original immature kerogen sample to that measured on the individual pyrolysed samples. The TR attains a value of 0.55 for the longest heated sample (840 h), showing that about 55 % of the labile organic matter in this sample, i.e., the fraction of organic matter that is susceptible to thermal transformation into hydrocarbons during maturation (Tissot & Welte, 1984), has undergone conversion into hydrocarbons compared to the original immature kerogen (Fig. 3B).

3.2. Mercury and Hg/TOC in residues, organic extracts, and oils

The results of the pyrolysis experiments show a net loss of Hg, corresponding to a decrease of ~ 65 % of the original yield in sub-samples with the greatest proportion of transformed organic matter (Fig. 4C). Similar to Hg concentration, the Hg/TOC values for the sub-samples also show a decreasing trend due to the relatively large variation of Hg concentration compared to more limited TOC change (e.g., ~65 % loss for Hg *vs* ~ 30 % loss for TOC, Fig. 3A), and particularly the pronounced Hg loss in the first 24 hrs. As organic-matter conversion progresses, the interpretation of Hg/TOC could become complicated because of progressive Hg and TOC loss at different rates.

The results of Hg measurements in the bitumen from pyrolysis are shown in Table 4. Hg contents of Posidonienschiefer-derived oils range from 2.5 – 5.2 ppb (Indraswari et al., 2024), which is at the lower end of the range of Hg reported in oils globally (1 – 20 ppb; Wilhelm et al., 2007; Wilhelm and Bloom, 2000). The Hg concentrations in the Posidonienschiefer-derived oils appear to show a strong correlation with the polar and heteroatomic fraction of Lower Saxony Basin oils analysed in Stock and Littke (2016) using saturate, aromatic, resin and asphaltene (SARA) chromatography analyses (Fig. 6). This relationship between Hg and polar and heteroatomic fraction of the oils suggests that the association is mainly with the nitrogen, sulphur and oxygen (NSO) containing heteroatomic compounds in the heavy fraction, as previously observed by Wilhelm et al. (2006). These results, and the data from the Posidonienschiefer-derived oils in our experimental pyrolysis study, suggest that Hg can be mobilised in a liquid hydrocarbon fraction, particularly at the stage of peak oil generation where NSO and polar compounds are still present in abundance. Although the Hg concentrations in the bitumen from the artificially matured sediments are higher (average ~ 50 ppb) than the natural oils, these levels are still below the bulk value of the immature sediment (74.6 ppb). The greatest proportion of Hg (≥ 99 %) in the artificially matured sediments appears to be held in the sediment residue or escapes as released gases (Table 2; Fig. 5). The gas loss is calculated using the difference: Hg loss as gas = 100 % − %Hg in bitumen − %Hg in the sediment residue. To calculate these values, Hg

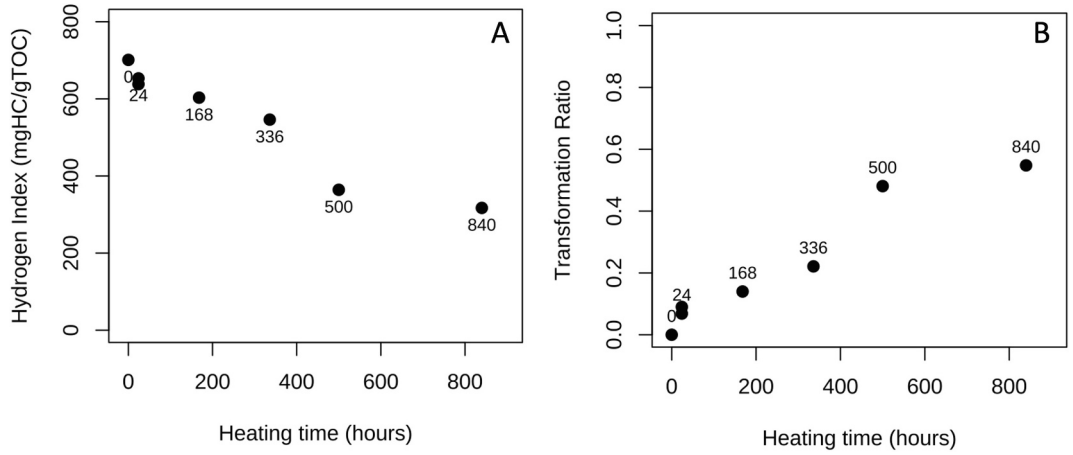

Fig. 3. Bulk organic geochemical results. (A) Hydrogen Index (HI) *versus* heating time in hours showing decreasing hydrogen content/conversion of kerogen into hydrocarbons during maturation; (B) Transformation Ratio (TR) *versus* heating time in hours showing how much organic matter (kerogen) has undergone primary cracking into hydrocarbons. Number labels by points show heating time in hours.

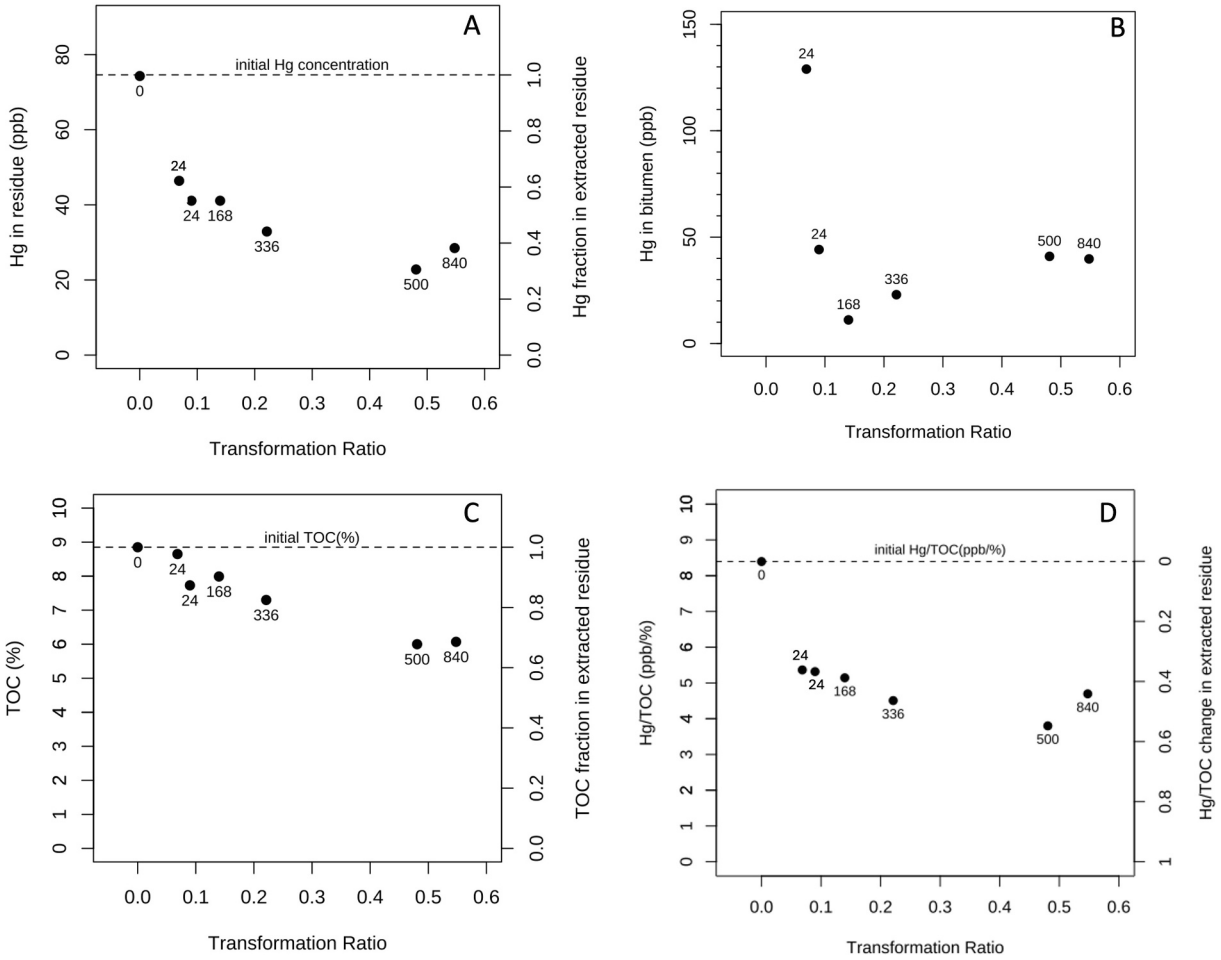

Fig. 4. (A) Total Hg concentration and fraction of Hg remaining of the original Hg concentration of the sub-samples (dashed line, 74.6 ppb) in the extracted sediments after artificial maturation. (B) Total Hg concentration in the produced bitumen. (C) As panel A and B with TOC in the residue (dashed line, 8.85 %). (D) Hg/TOC in the residue (dashed line, 8.43 ppb/%). Number labels by points show heating time in hours.

concentrations (in ppb) from the bulk rock sample, the heated sediment residue, and the extracted bitumen were used to determine the mass of Hg in each fraction. The remaining mass—assumed to be lost as gas—was then expressed as a percentage of the initial Hg content in the bulk rock sample.

3.3. Thermal Desorption Profiles from pyrolysis experiments and natural samples

Thermal desorption profiles (TDPs) of sub-samples from pyrolysis experiments reported here can be compared with averaged TDPs from

Table 4
Geochemical data from the Posidonienschiefer analysed in this study (also shown in Fig. 2). HI: Hydrogen Index. TOC: Total Organic Carbon. T_{max}: temperature of maximum hydrocarbon yield during pyrolysis. TR: transformation ratio (change in Hydrogen Index during pyrolysis). Extracted Residue: pyrolysed bulk rock residue after solvent extraction. Bitumen: the total solvent-extractable organic matter. The gas loss is calculated using the difference: Hg loss as gas = 100 % − %Hg in bitumen − %Hg in the sediments.

Heating time (hours)	HI	TOC (%)	T_{max} (°C)	TR	Bitumen (mg/g sediment)	Hg				
0	701	8.85	437	0	0.44	74.6 ppb				
						Extracted Residues		Bitumen		Loss (as gas)
						ppb	% of total Hg	ppb	% of total Hg	% of total Hg
24	653	8.65	436	0.07	3.16	48.00	64.34	128.95	0.36	35.29
24	638	7.73	440	0.09	9.02	41.10	55.09	44.15	0.38	44.53
168	603	7.99	440	0.14	11.58	41.45	55.56	11.10	0.04	44.40
336	546	7.3	441	0.22	14.89	33.05	44.30	22.95	0.33	55.36
500	364	6	443	0.48	22.58	22.55	30.23	40.95	1.00	68.77
840	317	6.07	440	0.55	18.31	28.50	38.20	39.75	0.76	61.04

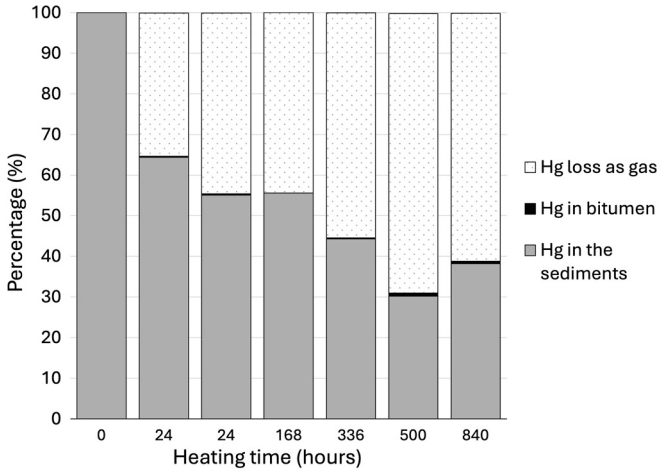

Fig. 5. Distribution of Hg in pyrolysis experiments showing Hg loss in the samples heated for longer periods of time. Mercury in bitumen does not show a clear trend with maturation. The gas loss is calculated using the difference of mass balance: Hg loss as gas = 100 % − %Hg in bitumen − %Hg in the sediment residue.

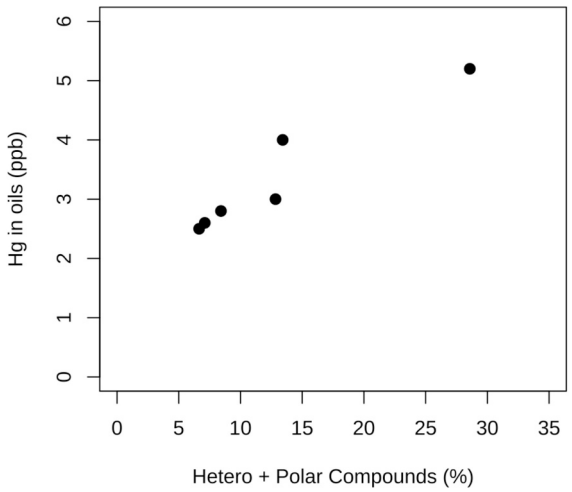

Fig. 6. Hg concentration in Posidonienschiefer-derived oils (data from Indraswari et al., 2024) showing a strong correlation with the polar and heteroatomic fraction of the oils (data from Stock & Littke, 2016), suggesting, for the Lower Saxony Basin, that the association is mainly with the NSO compounds in the heavy fraction (as also observed by Wilhelm et al. (2006)).

naturally matured samples, 5 samples from different depths (± 1 m from relative depth 34.65 m) each in the Posidonienschiefer from Cores B and C (Indraswari et al., 2024) and stratigraphically equivalent to the Core A used in all pyrolysis experiments. The TDPs of these two different sample sets (artificially and naturally matured) are presented in Fig. 7. It is important to note that the thermal maturity achieved in our pyrolysis experiments (%Ro ~ 0.5 % to ~ 0.88 %) did not reach the higher levels of maturity observed in Core B (%Ro ~ 1.5 %) and Core C (%Ro ~ 3.5 %).

The original, bulk rock sample from Core A (PS-0, Fig. 7) display a dominant, single-phase Hg release early in the TDP. The position of this phase in the TDP suggests it might be associated with Hg bound to organic matter (OM) or OM-associated sulphides, as proposed by Frieling et al. (2024). By contrast, sub-samples with %Ro > 0.64 % exhibit more complex TDPs, indicating two-phase, or perhaps even more intricate, Hg release patterns, suggesting the presence of multiple Hg species (PS-5 and PS-6, Fig. 7A and 7B). The artificially matured sub-samples are distinguished from the immature original sediment by two key features: lower overall Hg concentrations (Table 2) and a shift from a single dominant release peak to release patterns with a more pronounced 'shoulder' and bimodal peaks (Fig. 7A and 7B).

The naturally matured samples from Cores B and C differ from the artificially matured sub-samples, exhibiting higher Hg concentrations and peaks that appear later in the TDP (Fig. 7C). A clear trend of delayed peak Hg release with increasing natural maturity is observed, progressing from Core A (at 26 s) to Core B (33 s) to Core C (40 s) (Fig. 7C and 7D). Though the Hg concentrations in Cores B and C are relatively similar, delayed Hg desorption with increasing maturation suggests progressive changes in Hg speciation may occur with increasing maturity even beyond the oil/gas window. Indeed, limited hydrocarbon generation is expected during the maturation from Core B (%Ro ~ 1.5 %, entering dry gas window) to Core C (%Ro ~ 3.5 %, overmature post-gas window) (Indraswari et al., 2024).

Moreover, the samples from Core B exhibit a more prolonged Hg release compared to material from both Core A and Core C, resulting in lower amplitude peaks in area-normalised Hg (Fig. 7D). The variation in release duration and the shift towards later Hg release across the different sample sets (from Core A to Cores B and C) underscore the possibility that there may be appreciable and predictable Hg speciation

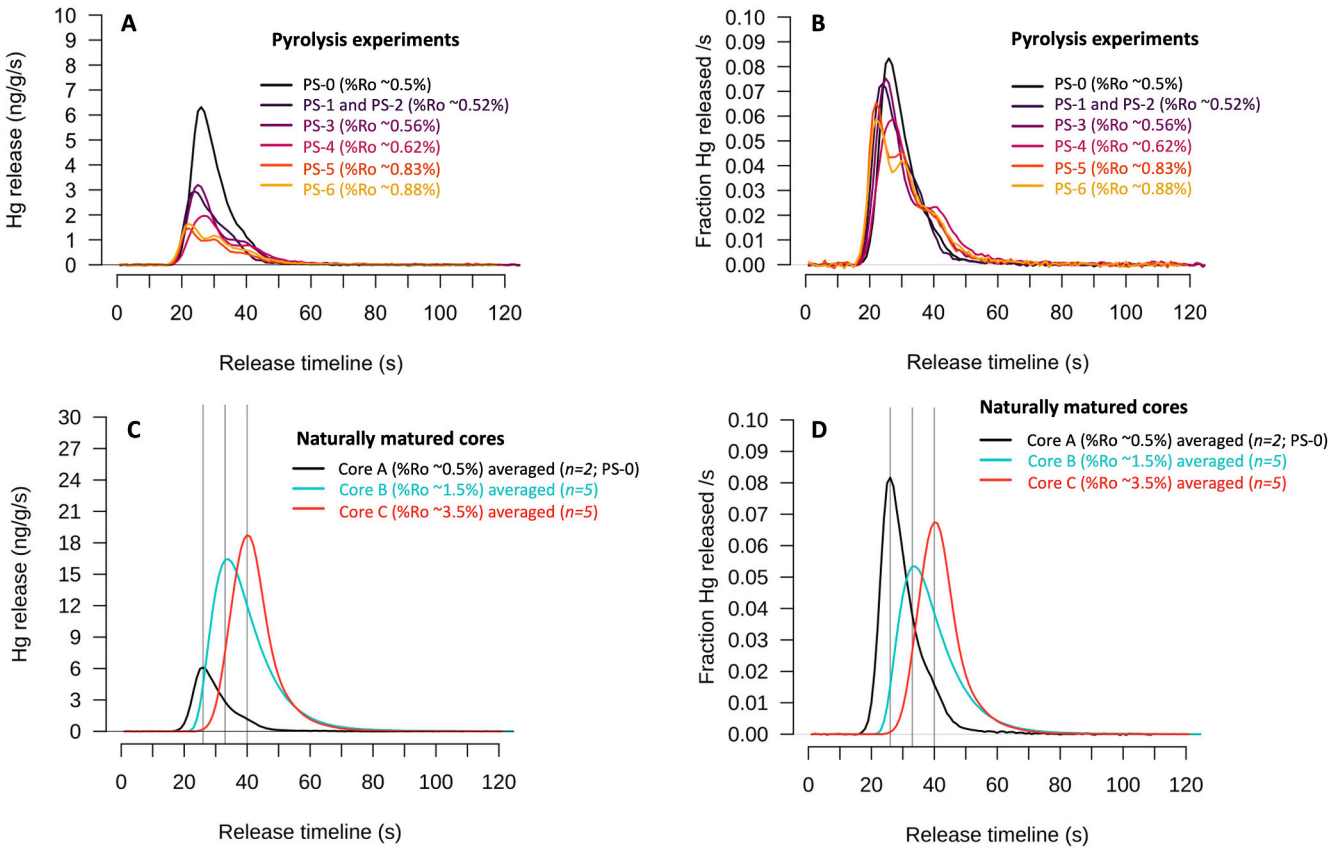

Fig. 7. Thermal desorption profiles of artificially matured sub-samples from pyrolysis experiments and naturally matured samples from Cores B and C. **(A)** Hg release rate per second for artificially matured sub-samples from Core A (PS-0) in pyrolysis experiments. **(B)** Fraction of total Hg released per second) for pyrolysis sub-samples. **(C)** Hg release rate per second for samples selected from Cores A, B, and C. **(D)** Average Hg release intensity normalised to total release for samples selected from Cores A, B, and C. Peak Hg release shifts from 26 s in averaged PS-0 (bulk rock sample from Core A used in this study) to 33 s in averaged samples from Core B and 40 s in averaged samples from Core C selected in this study (grey vertical lines on each peak), observed in both the total release and normalised plots.

changes with increasing maturity.

3.4. Mercury behaviour during cooling – reabsorption experiments

Upon opening a sub-sample at the highest temperature at 280 °C (0 min of cooling, inside the oven with the door open), a significant decrease in Hg concentration in the residue was observed, indicating substantial Hg loss as a gas phase (Fig. 8). Specifically, Hg concentrations remaining in the residue were 32 % and 26 % of the bulk rock sub-sample value when opened at 280 °C (0 min) and 211 °C (1 min), respectively. Subsequent openings after sealed cooling to 63 °C (4 min) and 16 °C (16 and 60 min at room temperature) showed Hg concentrations returning to 38 %, 66 %, and 96 % of the original values, suggesting appreciable and ultimately near complete Hg recapture at lower temperatures, from a gas phase, into sediments.

In the TDPs from the reabsorption experiments, the Hg release peaks for PS-0 (bulk rock), R-4 (sub-sample opened after 4 minutes of cooling), and R-16 were consistently observed at 26 s (Fig. 8B). By contrast, the peak Hg release for R-0 and R-1 are more extended, similar to the artificially matured sub-samples that were not allowed to cool down (§3.3). Regarding the Hg fraction release profiles (Fig. 8C), the curves for PS-0 (bulk rock), R-16 and R-60 were nearly identical, overlapping each other.

4. Discussion

4.1. Trends in Hg and processes driving Hg loss

We observed Hg loss across all isothermal maturation experiments, with the most pronounced decrease occurring within the first 24 h (Fig. 4A). Mercury concentrations in bitumen were found to be low (≤ 1 % of total initial Hg) while Hg in the gas phase (Hg lost during opening inferred by difference, see §3.2) was significant (>35 % of total initial Hg) (Table 4, Fig. 5). This result indicates that, under these experimental conditions, most of the mobilised Hg is present in the gas phase rather than in the bitumen after maturation. The low solubility of Hg in liquid hydrocarbons (see Wilhelm et al., 2007; Wilhelm and Bloom, 2000) likely contributes to its limited partitioning into bitumen. Field data from hydrocarbon production systems (e.g., Grotewold et al., 1979; Zettlitzer et al., 1997) further support the presence of Hg in natural gas phases under reservoir temperatures.

The pyrolysis temperature used in our experiments (325 °C) would allow the decomposition of the most common sedimentary Hg host species, such as organic matter and sulphide, followed by subsequent release as gas from the sediments. Previous studies have shown Hg desorption from sediments occurring at temperatures as low as ~ 150 °C (Rumayor, et al., 2015a; Saniewska and Bełdowska, 2017). Other potentially relevant sedimentary Hg species that may decompose below the experimental pyrolysis temperature experienced by the sample include pyrite-bound Hg and HgS (Rumayor et al., 2015b, 2016).

Similar to previous experimental studies (Liu et al., 2022; Chen et al., 2022), we observe Hg loss with heating. This loss likely begins with the thermal reduction of mercury species to elemental Hg^0 during heating, which then volatilizes and escapes as gaseous mercury when the hot, sealed tubes are opened. The maximum Hg loss observed in this study (35–69 %) is lower than the Hg losses reported in Liu et al. (2022), which exceeded 99 % at their maximum temperature of 610 °C, and in Chen et al. (2022), which reached 76 % Hg loss at their maximum

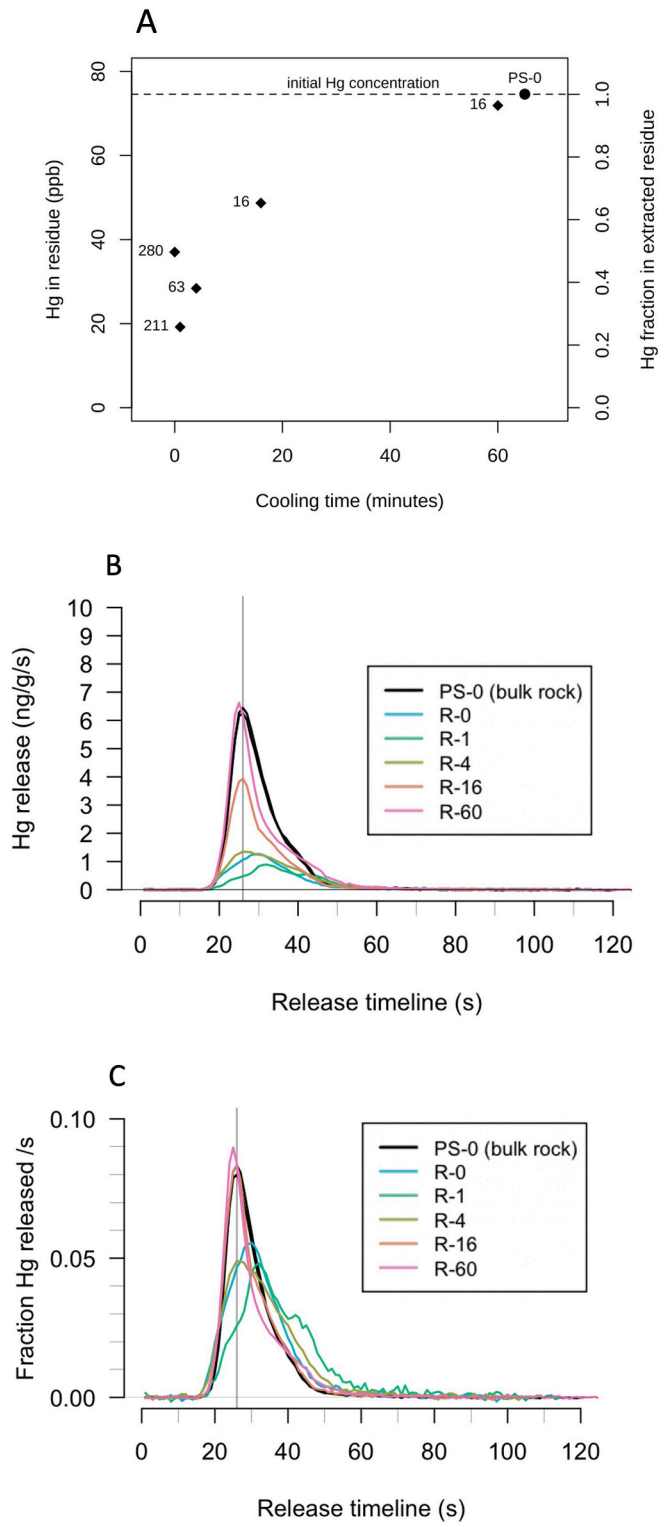

Fig. 8. (A) Mercury concentration and fraction of original Hg concentrations from reabsorption experiments with progressive cooling (filled diamonds). Number labels by points show opening temperature in °C. The top right point (filled dot) represents the bulk rock sub-sample (PS-0). (B) Thermal desorption profile for reabsorption experiments. (C) Average release intensity normalised to total Hg release. Grey vertical line in panel B and C shows peak Hg release of PS-0 (bulk rock), R-4, and R-16 at 26 s.

temperature of 700 °C. However, when examining similar temperature points, the findings become more comparable, with Hg losses ranging from 5–25 % at 300 °C (at 0.3 GPa) for Chen et al. (2022), and 30–65 % at 350 °C for Liu et al. (2022). Altogether, the experiments are, however, difficult to compare in detail even at similar temperature settings because they include a number of different conditions/set-ups used for the experiments (Table 1) and they used different lithologies containing possible different Hg phases with different thermal stability characteristics.

Besides the differences in temperature regime, we find that sample-specific Hg speciation is a likely candidate to explain the substantial differences in the behaviour for various shales in Liu et al. (2022) and Chen et al. (2022) for experiments conducted at the same temperature (experiments become more similar $\geq$ 450 °C because of complete Hg loss). Mercury speciation therefore can be a crucial factor in Hg mobilisation, as is the overall openness of the system and pressure (sealed tubes *vs* semi-closed anvil cell), that might impact Hg loss and reabsorption potential. Further, we note that some materials of the maturation vessels used in previous experiments (gold tubes in Liu et al., 2022; graphite in Chen et al., 2022) might be more conducive to absorbing Hg from a gas phase compared to the glass used in our experiments (e.g., gold-amalgamation used in direct Hg analysers: Schroeder, et al., 1985; Lee & Park, 2003). Altogether, we find the results for Hg loss are broadly comparable to previous works and not unexpected given the temperature regime employed here.

4.2. Mercury partitioning into (hydrocarbon) fluid and gas phases

As kerogen cracks and forms bitumen and a mobile fluid phase, Hg associated with organic matter may selectively move to specific organic fractions (e.g., polar, asphaltene-fractions and natural gas condensates) (Wilhelm et al., 2006). Interestingly, Hg did not show a strong tendency to partition into the extractable (oil) phase, with the concentration of Hg in extracted hydrocarbons typically at or below the sediment average (Table 2). It follows that the Hg/TOC of the bitumen ($\leq$ 1.5 ppb/%, with bitumen contains typically ca. 82–87 % C by mass, Berkowitz, 1997) is below that of the immature sediment used here (8.43 ppb/%). These data imply that only a very small fraction ($\leq$1%) of the total Hg present in the sediment is hosted in the extracted bitumen. In contrast to the Hg in bitumen, Hg in the gas phase (potentially as Hg^0) is lost from the artificially matured sub-samples upon opening the hot tubes and this process appears to be the dominant pathway for removal of mobilised Hg in these experiments. To what extent this experimental process replicates Hg dynamics in burial-driven thermal maturation is less certain, as temperature is likely to be a strongly controlling factor in Hg mobility and the majority of sedimentary Hg species would not be stable at the temperatures employed here (325 °C). However, the observations from our experiments may become more relevant near igneous intrusions, which also produce hydrocarbons (e.g., Svensen et al. 2015) and mobilised Hg (e.g., Liu et al. 2022, Svensen et al. 2023a), both of which can migrate out of contact aureoles. The limited partitioning into liquid hydrocarbons or other solvent-extractable fractions in our experiments suggests that Hg would likely experience limited transport by hydrocarbons in contact aureoles, and that Hg transport might be dominated by the gas phase in such settings.

4.3. Mercury reabsorption from a gas phase

In a previous study of the same Posidonienschiefer sequences from the Lower Saxony Basin, we observed a 2- to 3-fold increase in Hg concentrations and Hg/TOC due to burial-related maturation of sediments compared to the more immature stratigraphic equivalent section (Indraswari et al., 2024). We attributed the increase in Hg concentrations in the natural system to loss of rock mass, particularly TOC and water and perhaps subtly elevated original sedimentary Hg concentrations. In most sediments, loss of rock mass during maturation would be

relatively small but in organic-rich shales mass loss may have influenced a significant fraction of the total rock mass, which implies that, if Hg is effectively immobile during thermal maturation, Hg concentrations increase through the closed-sum effect. There is also the possibility that Hg was temporarily partitioned into a gas or fluid phase but ultimately remained in the host-rock, reabsorbed with residual organic-matter fractions or sulphides, its mobility being limited primarily by the very low permeability of the Posidonienschiefer.

In our experiments at 325 °C, a substantial proportion of the original Hg was initially desorbed from sediments and moved into a gas phase. The simple reabsorption experiments conducted here serve to illustrate the fate of mobilised (gaseous) Hg during cooling, and to test whether the result may match the observations from burial or igneous heating. Remarkably, we find that a substantial part of the desorbed, gaseous, Hg is recaptured in the sediment after only a very limited time (minutes) at lower temperature. Moreover, most of the recaptured Hg is not extractable with organic solvents (Sup. Table S1), effectively excluding the possibility that it has been taken up into hydrocarbons or formed (thermogenic) methylmercury (Zettlitzer et al., 1997, Wilhelm et al., 2006). Finally, a heating experiment where we exposed the sub-samples marked by Hg recapture overnight at 80 °C in an open vessel showed no concentration changes. This experiment excludes the presence of appreciable amounts of extremely volatile Hg species, such as condensed Hg^0 (e.g., Windmöller et al. 1996). We therefore argue that volatilised Hg (likely gaseous Hg^0) can be rapidly re-oxidised and efficiently reabsorbed into or onto organic particles and sulphides after cooling; an observation that seems to align with previous observations of retained Hg in thermally altered rocks around igneous intrusions (Frieling et al., 2025).

4.4. *The potential impact of Hg speciation and changes in Hg speciation: natural system vs artificial maturation*

The response of sedimentary Hg to heating and maturation can vary significantly across different shales (terrestrial *vs* marine *vs* lacustrine organic matter), as demonstrated in Liu et al. (2022). These variations may, in part, be attributed to differences in the nature of the chemical species of Hg present in the shales. The results obtained from the naturally matured Core B and C samples (Fig. 7 C, D), as well as the experimental data (Fig. 7A, B), suggest that during burial-maturation Hg speciation evolves with temperature and time, ultimately leading to a more significant proportion of temperature-resistant species. This suggestion could imply that processes accompanying burial maturation, such as pyritization, may limit Hg mobility during and after hydrocarbon formation.

While helpful in understanding Hg mobilisation and phase transformation at high temperatures, the controlled condition of artificial maturation experiments thus cannot fully replicate the complexities of natural burial maturation. These experiments lack the extended timescales and pressures characteristic of natural burial maturation and are conducted at slightly higher temperatures than would occur in the hydrocarbon window. These practical compromises required by artificial maturation experiments result in Hg behaviour that appears to differ from the transformations observed in natural burial maturation. The differences in TDPs between our experimental and natural Posidonienschiefer sub-samples (Fig. 7) highlight the fact that our experiments probably cannot fully mimic Hg phase changes that occur during burial maturation.

However, we propose that our experiments better simulate certain processes driving Hg mobilisation and recapture in contact aureoles, such as the rapid release and reabsorption of gaseous Hg. The TDPs from our reabsorption experiments in this study (Fig. 8C, D), where Hg is recaptured as a low-temperature phase, are similar to shales observed in contact aureoles (Frieling et al., 2025).

5. Conclusions & Outlook

Artificial maturation experiments, designed to simulate the natural process of thermal transformation of labile organic matter, demonstrated a drop of (up to) ~ 65 % in Hg concentration with increasing heating time, mainly due to the release of volatilised gaseous Hg. Importantly, low Hg in bitumen extracted from the sediments indicates that Hg does not have a significant tendency to partition into hydrocarbon fluids produced during thermal maturation. After heating, only a minor fraction (≤1%) of initial Hg in the bulk rock sediments was transferred to the bitumen. In comparison, 64–30 % of initial Hg was retained in the rock residue, and 35–69 % lost as volatilised gas. Although this study did not conduct detailed speciation of organic sulfur compounds, sulfur-containing moieties are known to have a strong affinity for mercury. Future work could further characterize these species to better understand their role in mercury binding within hydrocarbon-bearing fluids and sediments.

Further, we studied the potential for Hg reabsorption during cooling using artificially matured sediments. These experiments showed that once mobilised, gaseous Hg in a closed system can be efficiently (≥95 %) reabsorbed back into the sediment within an hour during cooling to room temperature (16 °C).

While our experiments simulate some processes that drive mobilisation and recapture, we also find distinct differences between our experiments and burial-related naturally matured core shales. In particular, observed changes in Hg speciation with maturation suggest that, during burial maturation, mobilised Hg from organic matter may not reabsorb into a similar phase but, over time, progressively transition into more thermally stable phases. Using core material that represents various stages of burial-related maturation in the Posidonienschiefer (Lower Saxony Basin), we previously observed that Hg concentrations increased with maturity and loss of rock mass. Our new analyses suggest that the limited partitioning of Hg into bitumen and progressive transformation of Hg species into more thermally stable phases are processes that can limit Hg mobility both during and after hydrocarbon formation.

Together, the limited partitioning of Hg into bitumen and changing Hg speciation may explain the inefficient transport of Hg in the low-permeability and relatively low-temperature environments that generate hydrocarbons. However, our artificial maturation experiments perhaps more closely mimic the conditions in contact aureoles, particularly the rapid volatilisation and reabsorption of gaseous Hg. While our closed-system setup likely maintained reducing conditions due to organic-matter breakdown, natural fluid migration may involve interaction with more oxidising groundwater or meteoric fluids near the surface, potentially altering Hg mobility and retention. This complication represents an important area for future investigation, and hydrothermal vessel experiments could help better simulate redox gradients relevant to these (near-surface) processes.

In summary, our work demonstrates Hg behaviour in heated sediments is determined by temperature and rate of heating as well as cooling and differential mobility in open and closed systems. Our data show a limited partitioning into bitumen that aligns well with generally low Hg concentration in natural hydrocarbons. These factors are relevant to deep burial but are particularly important for sediments affected by igneous intrusions. We find that special attention must be paid when using Hg concentrations or Hg/TOC ratios as proxies of large-scale volcanism in geological history, especially Hg emissions that are inferred to result from reactions around igneous intrusions into sedimentary rocks.

7. Data Availability

Data are available through Figshare at https://doi.org/10.6084/m9.figshare.27257871.

CRediT authorship contribution statement

Asri O. Indraswari: Writing – original draft, Visualization, Investigation, Data curation, Conceptualization. **Joost Frieling:** Writing – review & editing, Validation, Supervision, Conceptualization. **Erdem Idiz:** Writing – review & editing, Validation, Resources, Conceptualization. **Tamsin A. Mather:** Writing – review & editing, Validation, Supervision, Funding acquisition, Conceptualization. **Hugh C. Jenkyns:** Writing – review & editing, Validation, Supervision, Conceptualization. **Stuart A. Robinson:** Writing – review & editing, Validation, Supervision, Conceptualization. **Alexander J. Dickson:** Writing – review & editing, Validation, Methodology, Conceptualization.

Declaration of competing interest

The authors declare that they have no known competing financial interests or personal relationships that could have appeared to influence the work reported in this paper.

Acknowledgments

We thank S. Wyatt, D. Hillegonds, and B. Linscott (University of Oxford) for analytical assistance. Funding was provided from the European Research Council Consolidator Grant (ERC-2018-COG-818717-V-ECHO). Special thanks to Shell Global Solutions B.V. for access to samples for this study. A.I. is supported by a Jardine Foundation scholarship.

Appendix A. Supplementary material

The supplementary material includes Table S1 of mercury (Hg) concentration data from sub-samples in reabsorption experiment in this study. Supplementary material to this article can be found online at https://doi.org/10.1016/j.gca.2025.07.001.

References

Behar, F., Beaumont, V., Penteado, D.B., H. l., 2001. Rock-Eval 6 Technology: Performances and Developments. Oil Gas Sci. Technol. 56 (2), 111–134.
Benoit, J.M., Mason, R.P., Gilmour, C.C., Aiken, G.R., 2001. Constants for mercury binding by organic matter isolates from the Florida Everglades. Geochim. Cosmochim. Acta 65 (24), 4445–4451.
Berkowitz, N., 1997. Chapter 5 - Composition and chemical properties. In: Berkowitz, N. (Ed.), Fossil Hydrocarbons. Academic Press, pp. 83–120.
Bin, C., Xiaoru, W., Lee, F.S.C., 2001. Pyrolysis coupled with atomic absorption spectrometry for the determination of mercury in chinese medicinal materials. Anal. Chim. Acta 447 (1–2), 161–169.
Bryndzia, L.T., Burgess, J.M., Bourdet, J., 2022. Predicting the Solubility of Mercury in Hydrocarbons. SPE J. 28 (02), 859–875.
Burnham, A.K., 2017. Pyrolysis in Closed Systems. In: Global Chemical Kinetics of Fossil Fuels. Springer International Publishing, Cham., pp. 205–272
Celestino, R., 2019. Environmental change and carbon cycling during the Early Jurassic: a multi-proxy study on the Posidonienschiefer of NW Germany, (Doctoral dissertation). University of Exeter, Retrieved from http://hdl.handle.net/10871/36576.
Chen, D., Ren, D., Deng, C., Tian, Z., Yin, R., 2022. Mercury loss and isotope fractionation during high-pressure and high-temperature processing of sediments: Implication for the behaviors of mercury during metamorphism. Geochim. Cosmochim. Acta 334, 231–240.
Dembicki, H., 2022. Chapter 2 - The formation of petroleum accumulations. In: Dembicki, H. (Ed.), Practical Petroleum Geochemistry for Exploration and Production (Second Edition), Elsevier, pp. 21–67.
Dickson, A.J., Idiz, E., Porcelli, D., Murphy, M.J., Celestino, R., Jenkyns, H.C., Poulton, S. W., Hesselbo, S.P., Hooker, J.N., Ruhl, M., van den Boorn, S.H.J.M., 2022. No effect of thermal maturity on the Mo, U, Cd, and Zn isotope compositions of lower Jurassic organic-rich sediments. Geology 50 (5), 598–602.
Dickson, A.J., Idiz, E., Porcelli, D., van den Boorn, S.H.J.M., 2020. The influence of thermal maturity on the stable isotope compositions and concentrations of molybdenum, zinc and cadmium in organic-rich marine mudrocks. Geochim. Cosmochim. Acta 287, 205–220.
Fendley, I.M., Frieling, J., Mather, T.A., Ruhl, M., Hesselbo, S.P., Jenkyns, H.C., 2024. Early Jurassic large igneous province carbon emissions constrained by sedimentary mercury. Nat. Geosci. 17 (3), 241–248.
Frieling, J., Svensen, H.H., Mather, T.A., 2025. Mercury efficiently volatilized but not removed from sediments around igneous intrusions. Geology 53 (2), 176–180.
Frieling, J., Fendley, I.M., Nawaz, M.A., Mather, T.A., 2024. Assessment of Hg Speciation changes in the Sedimentary Rock Record from thermal Desorption Characteristics. Geochem. Geophys. Geosyst. 25, e2024GC011502.
Frimmel, A., Oschmann, W., Schwark, L., 2004. Chemostratigraphy of the Posidonia Black Shale, SW Germany I. Influence of sea-level variation on organic facies evolution. Chem. Geol. 206 (3–4), 199–230.
Gluyas, J.G., Swarbrick, R.E., 2021. Petroleum geoscience. John Wiley & Sons.
Gorbanenko, O.O., Ligouis, B., 2015. Variations of organo-mineral microfacies of Posidonia Shale from the Lower Saxony Basin and the West Netherlands Basin: Application to paleoenvironmental reconstruction. Int. J. Coal Geol. 152, 78–99.
Gorbanenko, O.O., Ligouis, B., 2014. Changes in optical properties of liptinite macerals from early mature to post mature stage in Posidonia Shale (lower Toarcian, NW Germany). Int. J. Coal Geol. 133, 47–59.
Grasby, S.E., Them, T.R., Chen, Z., Yin, R., Ardakani, O.H., 2019. Mercury as a proxy for volcanic emissions in the geologic record. Earth Sci. Rev. 196, 102880.
Grotewold, G., Fuhrberg, H.-D., Philipp, W., 1979. Production and processing of nitrogen-rich natural gases from reservoirs in the NE part of the Federal Republic of Germany, 10th. World Petroleum Congress, Bucharest, Romania. WPC-18306.
Indraswari, A.O., Frieling, J., Mather, T.A., Dickson, A.J., Jenkyns, H.C., Idiz, E., 2024. Investigating the Behavior of Sedimentary Mercury (Hg) during Burial-Related thermal Maturation. Geochem. Geophys. Geosyst. 25, e2024GC011555.
Jones, M.T., Percival, L.M.E., Stokke, E.W., Frieling, J., Mather, T.A., Riber, L., Schubert, B.A., Schultz, B., Tegner, C., Planke, S., Svensen, H.H., 2019. Mercury anomalies across the Palaeocene–Eocene thermal Maximum. Clim. Past 15 (1), 217–236.
Lee, S.H., Park, Y.O., 2003. Gas-phase mercury removal by carbon-based sorbents. Fuel Process. Technol. 84 (1–3), 197–206.
Lewan, M.D., Winters, J.C., Mcdonald, J.H., 1979. Generation of oil-like pyrolyzates from organic-rich shales. Science 203 (4383), 897–899.
Li, X., Wang, Q., Zhang, W., Yin, H., 2016. Contact metamorphism of shales intruded by a granite dike: Implications for shale gas preservation. Int. J. Coal Geol. 159, 96–106.
Liu, Z., Tian, H., Yin, R., Chen, D., Gai, H., 2022. Mercury loss and isotope fractionation during thermal maturation of organic-rich mudrocks. Chem. Geol. 612, 121144.
Lu, S.-T., Kaplan, I.R., 1989. Pyrolysis of kerogens in the absence and presence of montmorillonite—II. Aromatic hydrocarbons generated at 200 and 300°C☆. Org Geochem. 14, 501.
O'Connor, L.K., Robinson, S.A., Naafs, B.D.A., Jenkyns, H.C., Henson, S., Clarke, M., Pancost, R.D., 2019. Late cretaceous Temperature Evolution of the Southern High Latitudes: a TEX86 Perspective. Paleoceanogr. Paleoclimatol. 34 (4), 436–454.
Outridge, P.M., Sanei, H., Stern, G.A., Hamilton, P.B., Goodarzi, F., 2007. Evidence for control of mercury accumulation rates in Canadian High Arctic Lake sediments by variations of aquatic primary productivity. Environ. Sci. Tech. 41 (15), 5259–5265.
Percival, L.M.E., Bergquist, B.A., Mather, T.A., Sanei, H., 2021. Sedimentary Mercury Enrichments as a Tracer of Large Igneous Province Volcanism. In: Ernst, R.E., Dickson, A.J., Bekker, A. (Eds)., Large Igneous Provinces. AGU, Geophysical Monographs, 255, pp. 247–262.
Percival, L.M.E., Jenkyns, H.C., Mather, T.A., Dickson, A.J., Batenburg, S.J., Ruhl, M., Hesselbo, S.P., Barclay, R., Jarvis, I., Robinson, S.A., Woelders, L., 2018. Does large igneous province volcanism always perturb the mercury cycle? Comparing the records of Oceanic Anoxic event 2 and the end-cretaceous to other Mesozoic events. Am. J. Sci. 318 (8), 799–860.
Percival, L.M.E., Witt, M.L.I., Mather, T.A., Hermoso, M., Jenkyns, H.C., Hesselbo, S.P., Al-suwaidi, A.H., Storm, M.S., Xu, W., Ruhl, M., 2015. Globally enhanced mercury deposition during the end-Pliensbachian extinction and Toarcian OAE: a link to the Karoo – Ferrar Large Igneous Province. Earth Planet. Sci. Lett. 428, 267–280.
Peters, K.E., Walters, C.C., Moldowan, J.M., 2004. The Biomarker Guide. Cambridge University Press.
Poetz, S., Horsfield, B., Wilkes, H., 2014. Maturity-driven generation and transformation of acidic compounds in the organic-rich Posidonia shale as revealed by electrospray ionization Fourier transform ion cyclotron resonance mass spectrometry. Energy Fuel 28 (8), 4877–4888.
Röhl, H.J., Schmid-Röhl, A., Oschmann, W., Frimmel, A., Schwark, L., 2001. The Posidonia Shale (lower Toarcian) of SW-Germany: an oxygen-depleted ecosystem controlled by sea level and palaeoclimate. Palaeogeogr. Palaeoclimatol. Palaeoecol. 165 (1–2), 27–52.
Rumayor, M., Diaz-Somoano, M., Lopez-Anton, M.A., Martinez-Tarazona, M.R., 2015a. Application of thermal desorption for the identification of mercury species in solids derived from coal utilization. Chemosphere 119, 459–465.
Rumayor, M., Lopez-Anton, M.A., Díaz-Somoano, M., Martínez-Tarazona, M.R., 2015b. A new approach to mercury speciation in solids using a thermal desorption technique. Fuel 160, 525–530.
Rumayor, M., Lopez-Anton, M.A., Díaz-Somoano, M., Maroto-Valer, M.M., Richard, J.-H., Biester, H., Martínez-Tarazona, M.R., 2016. A comparison of devices using thermal desorption for mercury speciation in solids. Talanta 150, 272–277.
Sanei, H., Grasby, S.E., Beauchamp, B., 2012. Latest Permian mercury anomalies. Geology 40 (1), 63–66.
Saniewska, D., Bełdowska, M., 2017. Mercury fractionation in soil and sediment samples using thermo-desorption method. Talanta 168, 152–161.
Schmid-Röhl, A., Röhl, H.J., Oschmann, W., Frimmel, A., Schwark, L., 2002. Palaeoenvironmental reconstruction of lower Toarcian epicontinental black shales (Posidonia Shale, SW Germany): Global versus regional control. Geobios 35 (1), 13–20.
Schroeder, W., Hamilton, M., Stobart, S., 1985. The use of noble metals as collection media for mercury and its compounds in the atmosphere. Rev. Anal. Chem 8 (3), 1.

Schwark, L., Frimmel, A., 2004. Chemostratigraphy of the Posidonia Black Shale, SW-Germany II. Assessment of extent and persistence of photic-zone anoxia using aryl isoprenoid distributions. Chem. Geol. 206 (3–4), 231–248.
Shen, J., Algeo, T.J., Chen, J., Planavsky, N.J., Feng, Q., Yu, J., Liu, J., 2019. Mercury in marine Ordovician/Silurian boundary sections of South China is sulfide-hosted and non-volcanic in origin. Earth Planet. Sci. Lett. 511, 130–140.
Shen, J., Feng, Q., Algeo, T.J., Liu, J., Zhou, C., Wei, W., Liu, J., Them II., T.R., Gill, B.C., Chen, J., 2020. Sedimentary host phases of mercury (Hg) and implications for use of Hg as a volcanic proxy. Earth Planet. Sci. Lett. 543, 116333.
Song, J., Littke, R., Weniger, P., 2017. Organic geochemistry of the lower Toarcian Posidonia Shale in NW Europe. Org Geochem. 106, 76–92.
Stock, A., Littke, R., 2016. Geochemical composition of oils from the Gifhorn Trough and Lower Saxony Basin in comparison to Posidonia Shale source rocks from the Hils Syncline Northern Germany. German Journal of Gastroenterology. 167 (2–3), 315–331.
Svensen, H.H., Planke, S., Neumann, E.-R., Aarnes, I., Marsh, J.S., Polteau, S., Harstad, H. H., Chevallier, L., 2015. Sub-Volcanic Intrusions and the link to Global Climatic and Environmental changes. In: Breitkreuz, C., Rocchi, S. (Eds.), Physical Geology of Shallow Magmatic Systems. Springer, Cham, pp. 249–272.
Svensen, H.H., Jones, M.T., Percival, L.M.E., Grasby, S.E., Mather, T.A., 2023a. Release of mercury during contact metamorphism of shale: Implications for understanding the impacts of large igneous province volcanism. Earth Planet. Sci. Lett. 619, 118306.
Svensen, H.H., Jones, M.T., Mather, T.A., 2023b. Large Igneous Provinces and the Release of Thermogenic Volatiles from Sedimentary Basins. Elements 19 (5), 282–288.
Tannenbaum, E., Kaplan, I.R., 1985. Role of minerals in the thermal alteration of organic matter—I: generation of gases and condensates under dry condition*. Geochim. Cosmochim. Acta 49, 2589–2604.
Tissot, B.P., Welte, D.H., 1984. Petroleum Formation and Occurrence. Petroleum Formation and Occurrence, (2nd rev.). Springer-Verlag.
Wallace, G.T., 1982. The association of copper, mercury and lead with surface-active organic matter in coastal seawater. Mar. Chem. 11 (4), 379–394.
Wilhelm, S.M., Bloom, N., 2000. Mercury in petroleum. Fuel Process. Technol. 63 (1), 1–27.
Wilhelm, S.M., Liang, L., Cussen, D., Kirchgessner, D.A., 2007. Mercury in crude oil processed in the United States (2004). Environ. Sci. Tech. 41 (13), 4509–4514.
Wilhelm, S.M., Liang, L., Kirchgessner, D., 2006. Identification and Properties of Mercury Species in Crude Oil. Energy Fuel 20 (1), 180–186.
Windmöller, C.C., Wilken, R.-D., Jardim, W.D.F., 1996. Mercury speciation in contaminated soils by thermal release analysis. Water Air Soil Pollut. 89 (3–4), 399–416.
Zettlitzer, M., Scholer, H.F., Eiden, R., Falter, R., 1997. Determination of elemental, inorganic and organic Mercury in North German Gas condensates and formation brines. In: International symposium on oilfield chemistry, February 18–21, 1997, Houston, Texas.